Inactivation and Recovery of Sodium Currents in Cerebellar Purkinje Neurons: Evidence for Two Mechanisms

Indira M. Raman*† and Bruce P. Bean*

*Department of Neurobiology, Harvard Medical School, Boston, Massachusetts 02115, and †Department of Neurobiology and Physiology, Northwestern University, Evanston, Illinois 60208 USA

ABSTRACT We examined the kinetics of voltage-dependent sodium currents in cerebellar Purkinje neurons using whole-cell recording from dissociated neurons. Unlike sodium currents in other cells, recovery from inactivation in Purkinje neurons is accompanied by a sizeable ionic current. Additionally, the extent and speed of recovery depend markedly on the voltage and duration of the prepulse that produces inactivation. Recovery is faster after brief, large depolarizations (e.g., 5 ms at +30 mV) than after long, smaller depolarizations (e.g., 100 ms at −30 mV). On repolarization to −40 mV following brief, large depolarizations, a resurgent sodium current rises and decays in parallel with partial, nonmonotonic recovery from inactivation. These phenomena can be explained by a model that incorporates two mechanisms of inactivation: a conventional mechanism, from which channels recover without conducting current, and a second mechanism, favored by brief, large depolarizations, from which channels recover by passing transiently through the open state. The second mechanism is consistent with voltage-dependent block of channels by a particle that can enter and exit only when channels are open. The sodium current flowing during recovery from this blocked state may depolarize cells immediately after an action potential, promoting the high-frequency firing typical of Purkinje neurons.

INTRODUCTION

Voltage-dependent sodium currents in cerebellar Purkinje neurons have unusual kinetics. Following steps to positive potentials, during which sodium current activates and inactivates in a seemingly normal manner, repolarization to voltages in the range of −60 to −20 mV elicits a slowly rising, slowly decaying current (Raman and Bean, 1997). This resurgent current is carried by tetrodotoxin (TTX)-sensitive sodium channels, and single-channel recordings suggest that the same channels that carry resurgent current also produce conventional fast-inactivating current when they are activated by simple step depolarizations. These channels are probably formed by the NaV1.6 sodium channel α subunit (Burgess et al., 1995; Schaller et al., 1995; see Goldin, 1999 for nomenclature), as mutations that prevent expression of NaV1.6 in mice greatly diminish the resurgent current (Raman et al., 1997). The resurgent current is apparently elicited following action potential waveforms, and it probably contributes to the propensity of Purkinje neurons to fire spontaneous action potentials as well as all-or-none bursts of action potentials in response to brief stimulation (Raman and Bean, 1997, 1999a).

Here, we have examined the kinetics and voltage dependence of the resurgent current, with the goal of understanding its relation to conventional sodium channel gating. We propose a model of the underlying sodium channels in which there are two mechanisms of inactivation, a conventional mechanism from which channels recover through closed states and another mechanism involving voltage-dependent block of open channels by an endogenous particle. The second mechanism is favored by brief, large depolarizing steps, and resurgent current measured near −40 mV represents transient openings as channels recover from this blocked state and then enter the conventional inactivated state. In this model, resurgent current is analogous to the hooked tail currents produced by open channel blockers such as *N*-methyl-strychnine and pancuronium ions (Yeh and Narahashi, 1977; Cahalan and Almers, 1979; Armstrong and Croop, 1982).

MATERIALS AND METHODS

Cell preparation

Macroscopic sodium currents were recorded from neurons acutely dissociated from 14- to 20-day-old Black Swiss mice (Taconic Farms, Germantown, NY). Animals were anesthetized with methoxyflurane and decapitated. For isolation of Purkinje cells, the superficial layers of the cerebellum were removed and minced in ice-cold, oxygenated dissociation solution composed of (mM) 82 Na_2SO_4, 30 K_2SO_4, 5 $MgCl_2$, 10 HEPES, and 10 glucose and 0.001% phenol red (pH 7.4 with NaOH). The tissue was then incubated at 37°C in 10 ml of dissociation solution containing 3 mg/ml protease XXIII. During incubation, oxygen was blown over the surface of the fluid, and the fluid was gently stirred. After 7 min, the tissue was transferred to warm, oxygenated dissociation solution containing 1 mg/ml bovine serum albumin and 1 mg/ml trypsin inhibitor and minced further. The pieces were then transferred to Tyrode's solution composed of (mM) 150 NaCl, 4 KCl, 2 $CaCl_2$, 2 $MgCl_2$, 10 HEPES, and 10 glucose (pH 7.4 with NaOH) and triturated with a fire-polished Pasteur pipette to isolate individual neurons. Purkinje neurons were identified by their large somata and characteristic stump of the apical dendrite. The isolated Purkinje cell bodies are particularly suitable for voltage-clamp studies of sodium currents. The loss of the dendritic tree improves space clamp without greatly compromising currents, because of the relatively low dendritic density of

Received for publication 23 August 2000 and in final form 1 November 2000.

Address reprint requests to Dr. Indira M. Raman, Department of Neurobiology and Physiology, 2153 North Campus Drive, Northwestern University, Evanston, IL 60208. Tel.: 847-467-7912; Fax: 847-491-5211; E-mail: i-raman@northwestern.edu.

0006-3495/01/02/729/09 $2.00

sodium channels in Purkinje neurons (Stuart and Häusser, 1994). CA3 pyramidal cells were isolated with the same enzyme, inhibitor, and Tyrode's solutions, but hippocampal slices were cut on a tissue chopper and slices were incubated in enzyme. After washing with trypsin inhibitor, the CA3 regions of several slices were dissected out and triturated. Cells were used between 30 min and 5 h of trituration. All chemicals and drugs were obtained from Sigma (St. Louis, MO).

Whole-cell recordings

Voltage-clamp recordings were made with an Axopatch 200B amplifier (Axon Instruments, Foster City, CA). Borosilicate pipettes (1–3 MΩ) were wrapped with parafilm to minimize capacitance. Except as noted, pipettes were filled with a solution containing (mM) 117 CsCl, 9 EGTA, 9 HEPES, 1.8 $MgCl_2$, 14 Tris-creatine-PO_4, 4 MgATP, and 0.3 Tris-GTP (pH 7.4 with CsOH). Upon establishment of the whole-cell configuration, series resistance was generally less than 5 MΩ and was compensated by 85–95%. Cell capacitance ranged from ~15 to ~30 pF. Gravity-driven flow pipes were used to apply different solutions to the neurons. Cells were lifted and placed in front of a single barrel. Recordings of sodium currents were made in a reduced-sodium solution containing (mM) 50 NaCl, 110 TEA-Cl, 2 $BaCl_2$, 0.3 $CdCl_2$, and 10 HEPES (pH 7.4 with NaOH). Recordings were repeated in a solution of similar composition but including 300 nM TTX. The currents shown in all figures are TTX-sensitive sodium currents, isolated by subtracting the records obtained in TTX from those in TTX-free solutions. The quality of the voltage clamp was assessed by examining TTX-sensitive sodium currents evoked by step depolarizations in 2-mV increments from −90 mV (Raman and Bean, 1999b). Recordings that showed discontinuities in the peak current-voltage relation or inflections on the rising phase of the currents were excluded from the analysis. All recordings were performed at room temperature (20–22°C).

Acquisition and analysis

Data were acquired and analyzed with pCLAMP6 (Axon Instruments), Origin 4.5 (Microcal, Northampton, MA), and IgorPro 3.1 (Wavemetrics, Lake Oswego, OR). Data are plotted as mean ± SEM. Capacity transients resulting from imperfect TTX-subtraction have been blanked or reduced in most figures.

RESULTS

Fig. 1 *A* illustrates the basic phenomenology of resurgent sodium current in a mouse Purkinje neuron. Following a 5-ms depolarization to a positive potential (in this case +30 mV), repolarization evoked a surge of TTX-sensitive sodium current. This current is maximal on repolarization to potentials between −30 and −40 mV. Near −30 mV, the resurgent current rises in 5–6 ms and decays with an exponential time constant τ of 20–30 ms (Fig. 1 *B*). These kinetics are much slower than those of conventional sodium currents evoked by depolarizing steps, which rise in <0.3 ms and have a dominant decay τ near 1 ms. With repolarization to more negative potentials, the resurgent current is smaller, with an earlier peak (~1 ms at −60 mV) and faster decay ($\tau \approx 2$ ms at −60 mV).

The flow of resurgent current appears to be related to recovery from inactivation (Raman and Bean, 1997; Raman et al., 1997). The experiments shown in Fig. 2 explore this relationship. After conditioning steps to either +30 or −30 mV to promote inactivation, test pulses to 0 mV were used to assay the availability of sodium channels following a variable interval at −40 mV. Available channels include all channels that do not occupy inactivated states at the end of the interval, either because they are still open, because they never inactivated, or because they have recovered from inactivation. Following a 100-ms step to +30 mV, recovery was nonmonotonic, with availability reaching a maximum of 10% after 6 ms and then declining again to 5% after 40 ms (Fig. 2 *A*, *top*, and Fig. 2 *C*, *filled circles*). The time of maximum availability corresponded to the time of peak resurgent current flowing at −40 mV, and the decline of availability occurred in parallel with the decay of resurgent current. In contrast, following inactivation by a 100-ms step to −30 mV (Fig. 2 *A*, *bottom*), resurgent current was barely evident, and recovery from inactivation was minimal and monotonic (Fig. 2 *A*, *bottom*, and Fig. 2 *C*, *filled triangles*). This availability of ~4% at −40 mV is similar to that predicted by the steady-state availability curve, measured with 200-ms conditioning pulses (Fig. 2 *D*).

These results suggest the existence of two different types of inactivated states. Following accumulation in the state favored by the step to −30 mV, channels recover only

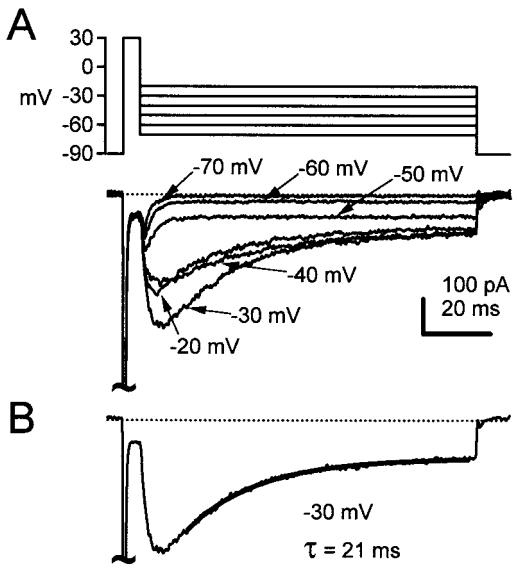

FIGURE 1 Resurgent sodium current in a mouse Purkinje neuron. (*A*) TTX-sensitive sodium currents were elicited in a Purkinje neuron by a 5-ms conditioning step to +30 mV, followed by step repolarizations to −70, −60, −50, −40, −30, and −20 mV, as indicated. Currents were signal-averaged from 3 runs, and the small leak and capacity current remaining in 300 nM TTX (signal-averaged from two runs) were subtracted. Internal solution contained 130 mM CsCl, 10 mM EGTA, 10 mM HEPES, pH 7.4 with CsOH. External solution contained 50 mM NaCl, 110 mM TEA-Cl, 2 mM $BaCl_2$, 0.3 mM $CdCl_2$, 10 mM HEPES, pH 7.4 with NaOH. In this and all figures of experimental data, truncated currents are indicated by a tilde. (*B*) The trace from *A* with repolarization to −30 mV is replotted. A single-exponential fit to the decay phase of resurgent current, with τ = 21 ms, is superimposed (*thick line*).

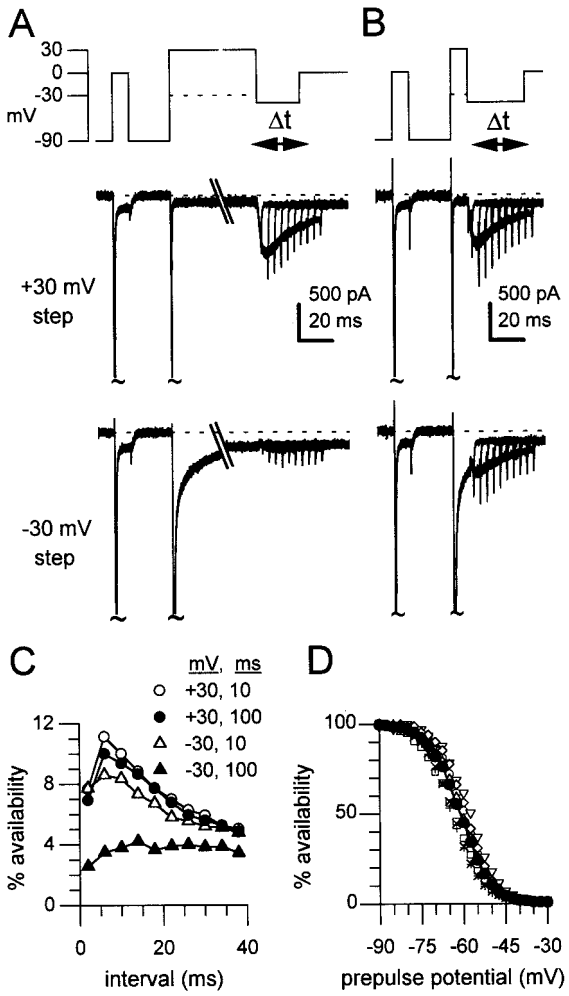

FIGURE 2 Recovery from inactivation and flow of resurgent current at −40 mV as a function of the potential and duration of the conditioning step. The voltage protocol in all recovery protocols includes a reference step to 0 mV, a 20-ms repriming interval at −90 mV (producing full recovery), a conditioning step to −30 mV or +30 mV, a variable recovery interval at −40 mV, and a test step to 0 mV. (*A*) Recovery after long conditioning steps. Break in traces, 50 ms. (*Top panel*) 100-ms conditioning step, either at +30 mV (*solid line*) or at −30 mV (*dashed line*). Recovery interval, −40 mV. (*Middle panel*) Following conditioning at +30 mV, recovery is nonmonotonic, and resurgent sodium current flows during the interval at −40 mV. (*Bottom panel*) Following conditioning at −30 mV, recovery is monotonic, and resurgent current is minimal during the recovery interval. (*B*) Recovery after brief conditioning steps. (*Top panel*) 10-ms conditioning step, either at +30 mV (*solid line*) or −30 mV (*dashed line*). (*Middle panel*) Following conditioning at +30 mV, recovery is nonmonotonic, and resurgent current flows during the interval at −40 mV. (*Bottom panel*) Following conditioning at −30 mV, the recovery profile and resurgent current are similar to those following the conditioning steps to +30 mV. (*C*) Percent availability, calculated as peak current elicited by the test step normalized by the peak current elicited by the reference step, is plotted against recovery interval for the four conditions in *A* and *B*. Legend indicates potential and duration of the conditioning step. Recordings are from a single neuron. (*D*) Quasi-steady-state availability, calculated as peak current evoked at 0 mV following a 200-ms conditioning step, normalized by the peak current at 0 mV following conditioning at −90 mV. Data for seven neurons are shown by *open symbols*. Average data (*closed, connected symbols*) indicate the predicted, steady-state recovery at each potential.

slightly at −40 mV, and little current accompanies the recovery. Following accumulation in the other state, favored by the step to +30 mV, substantial, rapid recovery occurs at −40 mV, accompanied by the resurgent current. However, this more substantial recovery is transient, decaying with a time course similar to the decay of the resurgent current.

A simple model that can account for these results is shown below, where C is the final closed state before opening, O is an open state, I is an inactivated state, and OB is a blocked state:

$$\rightarrow \rightarrow \rightarrow C \leftrightarrow O \leftrightarrow OB$$
$$\downarrow$$
$$I$$

In this scheme, I corresponds to normal inactivation, which is favored in the steady state at moderately negative potentials, near −40 mV. OB, in contrast, is primarily occupied following steps to +30 mV. On repolarization to potentials near −40 mV, channels in OB pass transiently through open and closed states, producing resurgent current, as well as rapid, partial recovery from inactivation, before equilibrating into the normal inactivated state.

We repeated the experiment of Fig. 2 *A* with briefer conditioning pulses of 10 ms. Recovery and resurgent current following brief conditioning steps at +30 were similar to those with long conditioning steps (Fig. 2 *B*, *top*, and Fig. 2 *C*, *open circles*). Surprisingly, however, following brief steps to −30 mV, resurgent current flowed during the recovery interval and produced a transient availability of ~9% (Fig. 2 *B*, *bottom*, and Fig. 2 *C*, *open triangles*). To some extent, both the ionic current and the sodium channel availability result from incomplete inactivation during the 10-ms pulse to −30 mV (at the end of which inactivation was still continuing). There was, however, an increase in sodium channel availability over the first 6 ms at −40 mV, corresponding to a rising phase in the ionic current. This result suggests that OB is occupied significantly after short steps to −30 mV as well as after either short or long steps to +30 mV.

We systematically tested the effect of potential and duration of a conditioning pulse on the subsequent production of resurgent current upon repolarizing to −30 mV (Fig. 3). Channels were conditioned at several potentials between −20 and +30 mV for short, medium, and long durations (2 ms, 20 ms, and 200 ms, respectively) and then repolarized to −30 mV to evoke resurgent current (Fig. 3 *A*). Resurgent current could be elicited upon repolarization from any potential but was larger following briefer steps to more positive potentials (Fig. 3 *B*; $N = 6$). This result suggests that the occupancy of OB is both voltage and time dependent. It is greatest soon after depolarization and decreases during sustained depolarization in a voltage-dependent manner.

As proposed above, the decay rate of the resurgent current may be determined by the time course with which

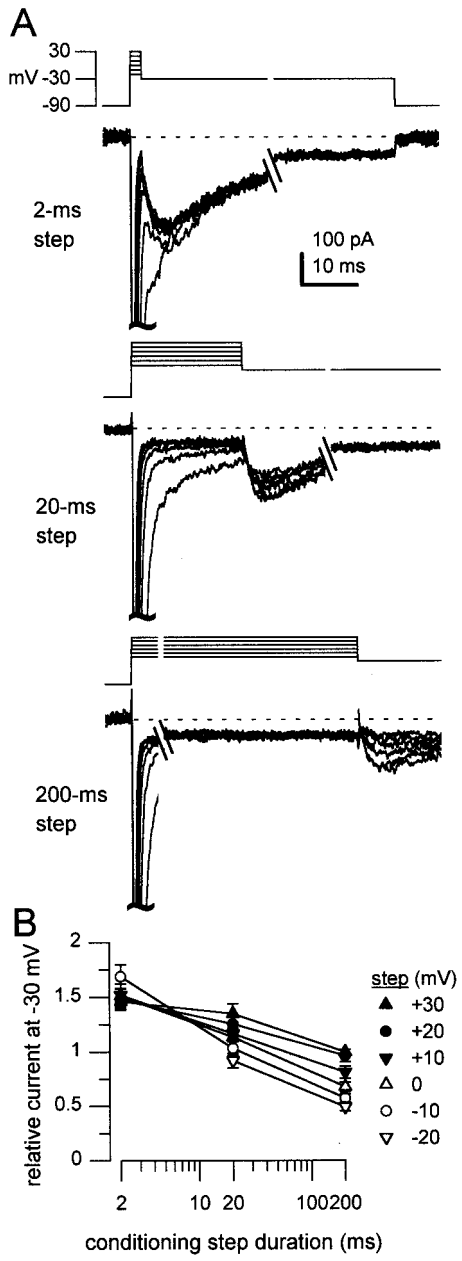

FIGURE 3 Dependence of resurgent current on amplitude and duration of voltage steps. (*A*) Voltage steps ranged from −20 to +30 mV (10-mV increments) for 2 ms (*top panels*), 20 ms (*middle panels*), or 200 ms (*bottom panels*). Break in top and middle panels, 30 ms; in bottom panels, 60 ms; repolarization potential, −30 mV. Current traces are plotted below the corresponding voltage protocols. Scale bars apply to all traces. Recordings are from a single neuron. (*B*) Relative maximal current upon repolarization, calculated as the peak current evoked upon repolarization normalized by the peak current evoked upon repolarization after the 200-ms conditioning step to +30 mV versus conditioning step duration. Mean data are from six cells. As evident in the top traces in *A*, incomplete inactivation after 2 ms at negative potentials overestimates the resurgent component of the current upon repolarization to −30 mV. For clarity, the current following 2 ms at −20 mV is not plotted.

channels in OB pass through O and C states and equilibrate in I. The experiment of Fig. 2 *B* (*bottom*) suggests that a similar process may occur even with a direct depolarization to a moderately negative potential, such as −30 mV. Specifically, channels may open, briefly enter OB, reopen, and accumulate in I. Such transitions might account for the bi-exponential decay of sodium currents after step depolarizations to −30 mV (Raman and Bean, 1997). Consistent with this idea, superimposition of currents evoked at −30 mV by depolarizations (from −90 mV) and repolarization (from +30 mV) showed converging slow phases of decay (Fig. 4).

When not voltage clamped, Purkinje cell bodies fire spontaneous action potentials at highly regular rates, with inter-spike intervals ranging across cells from ~5 to 50 ms (Raman and Bean, 1999a). The brevity and height of the action potentials (<2 ms half width, +15 mV peak) suggest that some sodium channels inactivating during the action potential will enter OB. After each action potential, the membrane repolarizes just beyond −60 mV before depolarizing to threshold (Raman and Bean, 1999a). To compare recovery from OB and I at inter-spike potentials, cells were conditioned for 5 ms at +30 mV or for 40 ms at −30 mV to maximize occupancy of OB or I, respectively. Recovery was then measured after various intervals at −60 mV, shown in Fig. 5 *A*. Recovery could be fit with a single exponential, with $\tau = 3.8$ ms following the step to +30 mV and 8.8 ms following the step to −30 mV (Fig. 5 *B*; $N = 5$). Although both conditioning steps inactivate the current nearly completely, the different recovery time courses support the idea that the channels are primarily occupying different states at the end of each conditioning step.

Between action potentials, the voltage is not constant, but depolarizing. To examine the effect of the rate of the inter-spike depolarization on the availability of sodium channels,

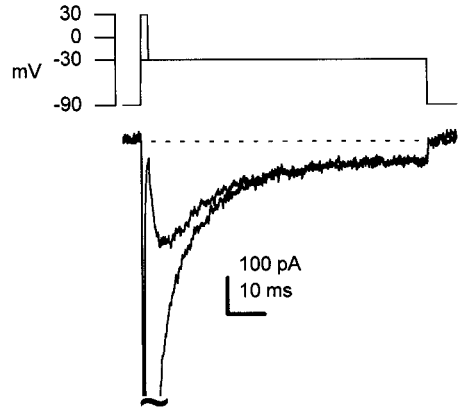

FIGURE 4 Decay phases of currents evoked by depolarizing and repolarizing voltage steps. Currents at −30 mV were evoked either by a direct depolarization from −90 mV or by a repolarization following a 2-ms step to +30 mV. The decay of the resurgent current (evoked by repolarization) matches the slow component of inactivation (evoked by depolarization).

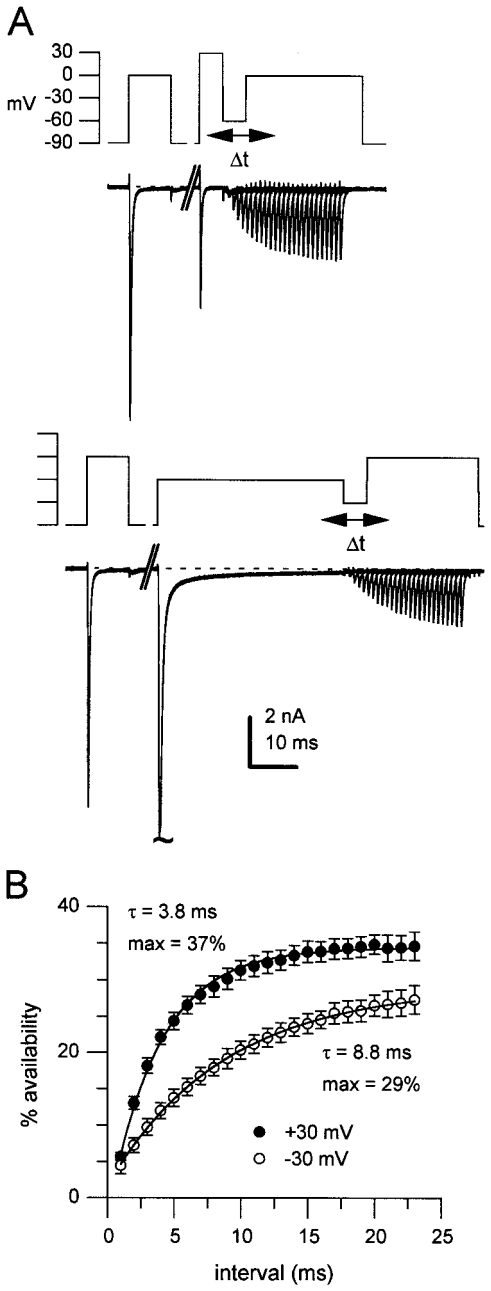

FIGURE 5 Time course of recovery from distinct inactivated states. (*A*) Recovery at −60 mV, measured following a 5-ms conditioning step to +30 mV (*upper panels*) or a 40-ms conditioning step to −30 mV (*lower panels*). Breaks in traces, 20 ms. Data are from a single neuron. (*B*) Percent availability after brief positive steps (*closed symbols*) and long, less positive steps (*open symbols*), calculated as peak current evoked by the test pulse normalized by the peak current evoked by the reference pulse versus recovery interval. Mean data ($N = 5$) are fitted with a single exponential function of the form % availability $= (A \exp(-t/\tau) + \%_{max})$, where $\%_{max}$ is the maximal availability, t is the interval in ms, τ is the time constant of recovery from inactivation, and $(\%_{max} + A)$ is the percentage of current that did not inactivate. Legend indicates conditioning pulse potentials.

we measured recovery from inactivation during voltage ramps. Following a 5-ms pulse to +30 mV, we ramped the membrane voltage from −60 to −50 mV at different rates during the recovery interval. The ramp durations varied from 6 to 36 ms, corresponding approximately to the range of inter-spike intervals we commonly observed in isolated cells (Raman and Bean, 1999a). This experiment is shown for a Purkinje neuron in Fig. 6 *A* (*left panel*). Interestingly, regardless of the ramp duration, the test pulse indicates a relatively fixed proportion of available sodium channels (~25%), varying by only 4% over all durations (Fig. 6 *B*; $N = 4$). During the ramp itself, a current flows, which probably includes resurgent current from channels exiting OB, as well as increasing activation of the currents that have recovered into closed (available) states. To see whether the availability profile correlates with the unusual kinetics of sodium channels in Purkinje cells, we repeated the experiments in CA3 pyramidal cells, which lack both resurgent current and recovery at moderately negative potentials (Raman and Bean, 1997). In this case, shorter ramps produced less availability, and there was no measurable current evoked in the ramp interval (Fig. 6 *A*, *right panel*, and 6 *B*; $N = 4$). These results suggest that, in Purkinje neurons, the dynamic redistribution among open, closed, and the OB states at inter-spike potentials maintains a relatively constant availability of sodium channels, a feature suitable for rapid repetitive firing of action potentials.

DISCUSSION

These experiments provide evidence that the resurgent current in Purkinje neurons is intimately related to development of inactivation and recovery from inactivation. When resurgent current flows, there is rapid, partial recovery from inactivation, and the speed and extent of the increase in availability following different conditioning steps is correlated with the ability of those steps to produce subsequent resurgent current. The decay of resurgent current at −30 mV has a nearly identical time course to the second, slow phase of decay of the sodium current elicited by a direct depolarization to −30 mV. These results can be accounted for if resurgent current results from the transient opening of channels during recovery from inactivation.

The inactivated state from which channels recover to produce resurgent current must be distinct from normal inactivated states, because during recovery from normal sodium channel inactivation, there is no flow of current and therefore no occupancy of open states. Armstrong and Croop (1982) specifically looked for a current during recovery from inactivation of sodium current in squid axons and showed that it was not present, and similar results were found with sodium current in hippocampal CA1 neurons (Kuo and Bean, 1994). Thus, recovery from the usual mechanism of sodium channel inactivation occurs through closed states, as if channels deactivate before recovering from

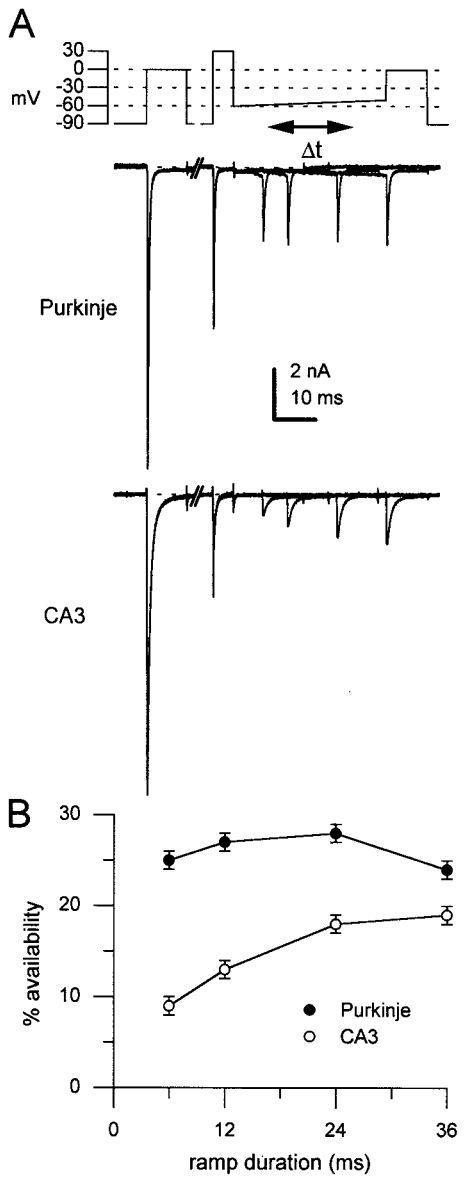

FIGURE 6 Recovery during voltage ramps, measured in cell types with and without resurgent current. (*A*) Conditioning pulses, +30 mV; breaks in traces, 20 ms. During the variable recovery interval, the membrane potential was ramped from −60 mV to −50 mV. Recordings are from a Purkinje neuron (*upper panels*) and from a CA3 hippocampal pyramidal neuron (*lower panels*). Note the faster inactivation kinetics during the steps to 0 mV in the Purkinje neuron. (*B*) Percent availability, calculated as peak current evoked by the test pulse normalized by the peak current evoked by the reference pulse, plotted against recovery interval. Purkinje neurons (*closed symbols*, $N = 4$) show an availability that remains relatively constant across recovery intervals and that is greater at all intervals than that of CA3 neurons (*open symbols*, $N = 4$).

inactivation (Kuo and Bean, 1994). This mechanism contrasts with recovery from N-type inactivation in Shaker potassium channels, where there is transient opening of channels during recovery (Demo and Yellen, 1991).

The simplest interpretation of the link between the inactivated state and the flow of resurgent current is a channel block by a particle that can enter and exit from the channel only when the channel is open. In fact, the phenomenology of resurgent current is essentially identical to the hooked tail currents that are seen during recovery from sodium channel block by compounds such as pancuronium, *N*-methylstrychnine, and azure A applied in the internal solution (Yeh and Narahashi, 1977; Cahalan and Almers, 1979; Armstrong and Croop, 1982). All of these are positively charged compounds that block open sodium channels in a highly voltage-dependent manner, and transient ionic current flows through the channel during recovery from block at hyperpolarized voltages.

A state model of sodium channel gating incorporating this interpretation is shown in Fig. 7. Normal activation and inactivation occur with transitions between the C, O, and I states, with voltage-dependent rate constants for activation and deactivation and voltage-independent rate constants for transitions between closed or open states and inactivated states. This model gives reasonable simulations of the voltage dependence of development of inactivation and recovery from inactivation for sodium channels that do not give resurgent current (Kuo and Bean, 1994). The second mechanism of inactivation is represented by the state called OB. Entry into this state occurs only from the open state in a voltage-independent manner, and exit occurs only to the open state, with a strongly voltage-dependent rate constant (e-fold change for 25 mV). The model in Fig. 7 is identical to the scheme given by Armstrong and Croop (1982) for block of sodium channels by azure A, except that the normal inactivation process is represented in an expanded form incorporating more inactivated states.

Figs. 8, *A* and *B*, shows the predictions of the model for the voltage protocols producing resurgent current and prepulse-dependent recovery from inactivation. On depolarization to +30 mV, most channels (~70%) move into OB immediately after opening. On repolarization, these channels pass back through the open state, producing resurgent current. The decay phase of resurgent current near −30 mV is due to movement of the open channels into normal inactivated states, whereas the faster decay phase at −60 mV is mainly due to deactivation of the open channels. The strong voltage dependence of the transition from OB to O accounts for the rapid recovery from inactivation observed experimentally after brief steps to +30 mV (Fig. 8 *C*).

The model in Fig. 7 assumes exclusivity between the two forms of inactivation; i.e., channels blocked by the hypothetical particle cannot also undergo normal inactivation, and vice-versa. In terms of the hinged-lid model for the molecular mechanism of normal inactivation, which envisions block of the inner mouth of the channels by the cytoplasmic linker connecting domains III and IV of the main α subunit of the sodium channel (West et al., 1992; Kellenberger et al., 1997), this would imply that occupancy of the channel by the blocking particle prevents binding of the linker.

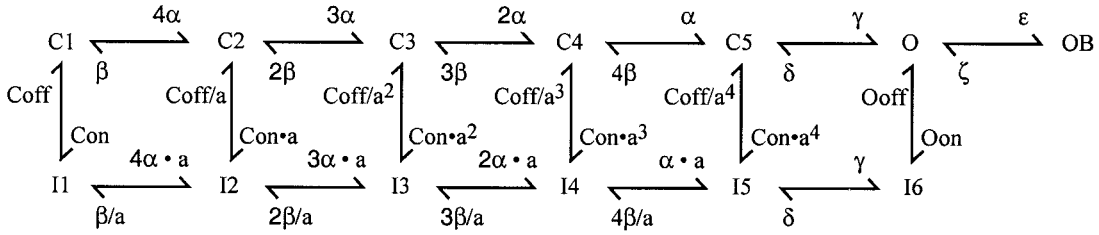

FIGURE 7 A model of resurgent sodium current. C1 to C5 denote sequential closed states and O denotes the open state. I1 to I6 denote the inactivated states for the normal mechanism of inactivation. The rate constants α, β, γ, and δ are (ms^{-1}): $150\exp(V/20)$, $3\exp(-V/20)$, 150, and 40, respectively. Con (0.005 ms^{-1}) and Coff (0.5 ms^{-1}) are the on and off rates for normal inactivation from the C1 state and are not voltage dependent. Oon (0.75 ms^{-1}) and Ooff (0.005 ms^{-1}) are the on and off rates for normal inactivation from the open state and are also independent of voltage. The factor a, which is equal to $[(\text{Coff}/\text{Con})/(\text{Ooff}/\text{Oon})]^{1/8}$, embodies progressively tighter binding of the normal inactivating particle as activation of channels is more complete. OB denotes the state entered by the second mechanism of inactivation, which is hypothesized to be equivalent to open channel block. The rate constant ϵ (1.75 ms^{-1}) is the voltage-independent rate constant for entry into this state, and ζ ($0.03\exp(-V/25$ ms^{-1}) is the voltage-dependent rate constant for exit from the state.

In the model, the steady state favors occupancy of the normal inactivated states rather than OB, as if binding of the hinged lid is tighter than that of the particle in OB. For example, the equilibrium between O and I6 yields only 0.6% occupancy of O, whereas the equilibrium between O and OB predicts 5% occupancy of O at −30 mV, 1.7% at 0 mV, and 0.5% at +30 mV. The favoring of normal inactivation seems required by the experimental results, because with longer conditioning steps to −30 mV and 0 mV, there is a progressive decline in the size of the resurgent current, as if channels slowly equilibrate out of OB and into I states (Fig. 3). The extent of this decline is less at +30 mV, consistent with OB and I states being equivalently absorbing at this voltage.

Purkinje neurons express multiple types of sodium channels, including NaV1.1, NaV1.2, and NaV1.6 (Vega-Saenz de Miera et al., 1997; Felts et al., 1997). Thus, the sodium currents we have recorded almost certainly represent the sum of currents from multiple types of channels. Most likely, virtually all of the resurgent current comes from NaV1.6 channels, as mice lacking expression of NaV1.6 channels have almost no resurgent current, although total peak transient sodium current with step depolarizations is reduced by only 40% (Raman et al., 1997). We have no way of knowing, however, just how much of the transient current comes from NaV1.6 channels. Presumably, at least 40% does, but it could be a larger fraction if in the NaV1.6 null mice there is compensatory upregulation of other channel types.

The hypothetical blocking particle could be part of the sodium channel proteins, or it could be part of the intracellular milieu. Interestingly, cloned NaV1.6 α subunits do not produce clear resurgent current when expressed in *Xenopus* oocytes (Smith et. al, 1998), suggesting that the blocking particle is not from the main sodium channel subunit protein. Similarly, NaV1.6 is apparently expressed in some cells, such as CA3 pyramidal neurons of the hippocampus and spinal neurons, which do not produce resurgent sodium current (Raman and Bean 1997; Pan and Beam, 1999). The possibility that the blocking particle is part of the NaV1.6 α subunit cannot be completely ruled out, however, because there are multiple alternatively spliced versions of the NaV1.6 protein, and the version expressed in Purkinje or other neurons is not known (Plummer et al., 1997). The blocking particle could also be from an accessory protein subunit, because the β subunit or subunits associated with the NaV1.6 α subunit in native cells is unknown and may differ from those ($\beta 1 + \beta 2$) used in the oocyte experiments (Smith et al. 1998).

Another possibility is that the blocking particle is a constituent of the intracellular solution. Two obvious possibilities are magnesium ions, which produce voltage-dependent, open channel block of inwardly rectifying potassium channels, and polyamines such as spermine and spermidine, which produce voltage-dependent block of inwardly rectifying potassium channels and, in neurons, glutamate receptor channels and acetylcholine receptor channels (Lopatin et al., 1994; Bowie and Mayer, 1995; Haghighi and Cooper, 1998). Magnesium does not appear to be the blocking particle, however, because the resurgent current was apparently unchanged when recordings were made with no magnesium in the intracellular solution ($N = 10$). In fact, the experiment in Fig. 1 was carried out using such a solution.

There is also some evidence against the blocking particle being a polyamine. Polyamines are present in *Xenopus* oocytes at sufficient concentrations to produce rectification in some inwardly rectifying potassium channels (Lopatin et al., 1994), yet the cloned NaV1.6 channel does not produce resurgent current when expressed in oocytes (Smith et al., 1998). Nevertheless, it is possible that the specific splice variant and subunit composition of this channel in Purkinje cells is different and allows block by endogenous polyamines.

Polyamine block of glutamate receptors can be reduced by large concentrations of intracellular ATP, which chelates polyamines (Watanabe et al., 1991; Ficker et al., 1994; Fakler et al., 1995; Bowie and Mayer, 1995). We therefore

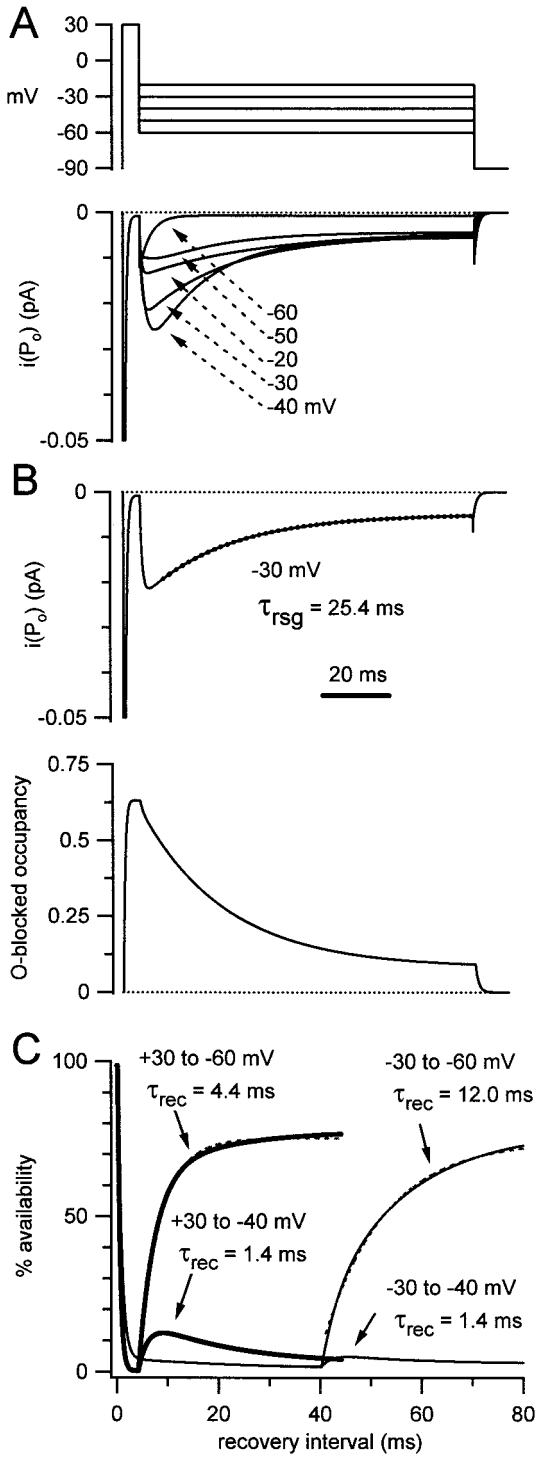

FIGURE 8 Simulations of resurgent sodium current. (*A*) Simulated currents (*lower panel*) in response to the voltage protocol (*upper panel*) consisting of a 5-ms conditioning step to +30 mV, followed by step repolarizations to −60, −50, −40, −30, and −20 mV, as indicated. The differential equations for transitions between states were integrated using a fourth-order Runge-Kutta algorithm implemented in IgorPro (WaveMetrics, Lake Oswego, OR). Step size for integration was 0.4 μs. If the expression for a voltage-dependent rate constant was greater than 6000 ms^{-1} at a given voltage, the rate constant was clipped to 6000 ms^{-1} to avoid instability. Current is plotted as the product of open probability, P_o, and unitary current, i, calculated for our experimental solutions with the Goldman-Hodgkin-Katz equation, assuming $P_{Cs} = 0.015\ P_{Na}$. (*B*) Simulated current (*top panel*) and occupancy of OB (*bottom panel*) for the −30-mV repolarization in *A*. The resurgent current at −30 mV was fitted with a single exponential with a decay time constant, τ_{rsg}, of 25.4 ms (*thick dashed line*). Time scale also applies to *A*. (*C*) Availability, simulated as the sum of all closed and open states, during and following conditioning steps of 5 ms at +30 mV (*thick traces*) and 40 ms at −30 mV (*thin traces*). After the conditioning steps, the simulated voltage was stepped to −60 mV or −40 mV, as labeled. Time courses of recovery were fitted with single exponentials (*dashed lines*), with time constants, τ_{rec}, as labeled.

tested for reduction of resurgent current with 10 mM ATP included in the intracellular solution, with inconclusive results. Under these recording conditions, resurgent current was not absent, but it seemed unusually small ($N = 5$). Conclusive results might require long periods of dialysis for effective equilibration of ATP into the cell, but this is made difficult by the limited lifetime of the preparation when recording with wide-tipped pipettes necessary to reduce series resistance.

One observation that fits well with a blocking particle that is part of the intracellular milieu is that in the mutant mice lacking expression of NaV1.6 (Burgess et al., 1995), resurgent current is reduced by ~90% but is not abolished (Raman et al., 1997). Thus, it is possible that such a blocker can produce some resurgent current by interacting with other types of sodium channels but has its largest effects on NaV1.6 channels, either because it has an intrinsically higher affinity for these channels or because normal inactivation competes less effectively.

Whatever the molecular mechanism, the type of inactivation associated with resurgent current produces effects on sodium channel activity that are likely to be physiologically significant. First, the buffering of channels by the OB state at voltages around −50 to −30 mV will tend to produce longer lasting occupancy of the open state than would otherwise occur. Effectively, this is a way of producing persistent sodium current at subthreshold voltages (see Crill, 1996), although such current would then represent dynamic redistribution of channels between OB, open, and normal inactivated states, rather than channels that simply fail to inactivate. It is consistent with the observation that sodium current elicited by slow voltage ramps (commonly used to define persistent current) and resurgent current are greatly reduced in mice lacking NaV1.6 (Raman et al., 1997). The idea of such a redistribution is also compatible with the original hypothesis of the physiological importance of persistent sodium current in Purkinje neurons (Llinás and Sugimori, 1980). A second physiologically important feature of the second mechanism of inactivation is that the open channel block not only terminates current flow, but also limits entry into absorbing inactivated states. Thus, when the block is relieved by repolarization, even to voltages near −40 mV, channels are readily available for reac-

tivation. The rapid availability of these channels (e.g., Fig. 5) is likely to facilitate the long-term, rapid firing that is characteristic of Purkinje cells (Granit and Phillips, 1956; Bell and Grimm, 1969; Latham and Paul, 1971; Llinás and Sugimori, 1980; Häusser and Clark, 1997; Raman and Bean 1997).

Supported by NS36855 (B.P.B.) and NS10396, NS39395 (I.M.R.). I.M.R. is a fellow of the Alfred P. Sloan Foundation and a Searle Scholar.

REFERENCES

Armstrong, C. M., and R. S. Croop. 1982. Simulation of Na channel inactivation by thiazine dyes. *J. Gen. Physiol.* 80:641–662.

Bell, C. C., and R. J. Grimm. 1969. Discharge properties of Purkinje cells recorded on single and double microelectrodes. *J. Neurophysiol.* 32: 1044–1055.

Bowie, D., and M. L. Mayer. 1995. Inward rectification of both AMPA and kainate subtype glutamate receptors generated by polyamine-mediated ion channel block. *Neuron.* 15:453–462.

Burgess, D. L., D. C. Kohrman, J. Galt, N. W. Plummer, J. M. Jones, B. Spear, and M. H. Meisler. 1995. Mutation of o new sodium channel gene, *Scn8a*, in the mouse mutant 'motor endplate disease.' *Nat. Genet.* 10:461–465.

Cahalan, M. D., and W. Almers. 1979. Block of sodium conductance and gating current in squid giant axons poisoned with quaternary strychnine. *Biophys. J.* 27:57–73.

Crill, W. E. 1996. Persistent sodium current in mammalian central neurons. *Annu. Rev. Physiol.* 58:349–362.

Demo, S. D., and G. Yellen. 1991. The inactivation gate of the Shaker K+ channel behaves like an open-channel blocker. *Neuron.* 7:743–753.

Fakler, B., U. Brandle, E. Glowatzki, S. Weidemann, H. P. Zenner, and J. P. Ruppersberg. 1995. Strong voltage-dependent inward rectification of inward rectifier K^+ channels is caused by intracellular spermine. *Cell.* 80:149–154.

Felts, P. A., S. Yokoyama, S. Dib-Hajj, J. A. Black, and S. G. Waxman. 1997. Sodium channel alpha-subunit mRNAs I, II, III, NaG, Na6 and hNE (PN1): different expression patterns in developing rat nervous system. *Brain Res. Mol. Brain Res.* 145:71–82.

Ficker, E., M. Taglialatela, B. A. Wible, C. M. Henley, and A. M. Brown. 1994. Spermine and spermidine as gating molecules for inward rectifier K^+ channels. *Science.* 266:1068–1072.

Goldin, A. L. 1999. Diversity of mammalian voltage-gated sodium channels. *Ann. N.Y. Acad. Sci.* 868:38–50.

Granit, R., and C. G. Phillips. 1956. Excitatory and inhibitory processes acting upon individual Purkinje cells of the cerebellum in cats. *J. Physiol.* 133:520–547.

Haghighi, A. P., and E. Cooper. 1998. Neuronal nicotinic acetylcholine receptors are blocked by intracellular spermine in a voltage-dependent manner. *J. Neurosci.* 18:4050–4062.

Häusser, M., and B. A. Clark. 1997. Tonic synaptic inhibition modulates neuronal output pattern and spatiotemporal synaptic integration. *Neuron.* 19:665–678.

Kellenberger, S., J. W. West, T. Scheuer, and W. A. Catterall. 1997. Molecular analysis of the putative inactivation particle in the inactivation gate of brain type IIA Na^+ channels. *J. Gen. Physiol.* 109:589–605.

Kuo, C. C., and B. P. Bean. 1994. Na^+ channels must deactivate to recover from inactivation. *Neuron.* 12:819–829.

Latham, A., and D. H. Paul. 1971. Spontaneous activity of cerebellar Purkinje cells and their responses to impulses in climbing fibres. *J. Physiol.* 213:135–156.

Llinás, R., and M. Sugimori. 1980. Electrophysiological properties of in vitro Purkinje cell somata in mammalian cerebellar slices. *J. Physiol.* 305:171–195.

Lopatin, A. N., E. N. Makhina, and C. G. Nichols. 1994. Potassium channel block by cytoplasmic polyamines as the mechanism of intrinsic rectification. *Nature.* 372:366–369.

Pan, F., and K. G. Beam. 1999. The absence of resurgent sodium current in mouse spinal neurons. *Brain Res.* 849:162–168.

Plummer, N. W., M. W. McBurney, and M. H. Meisler. 1997. Alternative splicing of the sodium channel SCN8A predicts a truncated two-domain protein in fetal brain and non-neuronal cells. *J. Biol. Chem.* 272: 24008–24015.

Raman, I. M., and B. P. Bean. 1997. Resurgent sodium current and action potential formation in dissociated cerebellar Purkinje neurons. *J. Neurosci.* 17:4517–4526.

Raman, I. M., and B. P. Bean. 1999a. Ionic currents underlying spontaneous action potentials in isolated cerebellar Purkinje neurons. *J Neurosci.* 19:1663–1674.

Raman, I. M., and B. P. Bean. 1999b. Properties of sodium currents and action potential firing in isolated cerebellar Purkinje neurons. *Ann. N.Y. Acad. Sci.* 868:93–96.

Raman, I. M., L. K. Sprunger, M. H. Meisler, and B. P. Bean. 1997. Altered subthreshold sodium currents and disrupted firing patterns in Purkinje neurons of Scn8a mutant mice. *Neuron.* 19:881–891.

Schaller, K. L., D. M. Krzemien, P. J. Yarowsky, B. K. Krueger, and J. H. Caldwell. 1995. A novel, abundant sodium channel expressed in neurons and glia. *J. Neurosci.* 15:3231–3242.

Smith, M. R., R. D. Smith, N. W. Plummer, M. H. Meisler, and A. L. Goldin. 1998. Functional analysis of the mouse Scn8a sodium channel. *J. Neurosci.* 18:6093–6102.

Stuart, G., and M. Häusser. 1994. Initiation and spread of sodium action potentials in cerebellar Purkinje cells. *Neuron.* 13:703–712.

Vega-Saenz de Miera, E., B. Rudy, M. Sugimori, and R. Llinás. 1997. Molecular characterization of the sodium channel subunits expressed in mammalian cerebellar Purkinje cells. *Proc. Natl. Acad. Sci. U.S.A.* 94:7059–7064.

Watanabe, S., K. Kusama-Eguchi, H. Kobayashi, and K. Igarashi. 1991. Estimation of polyamine binding to macromolecules and ATP in bovine lymphocytes and rat liver. *J. Biol. Chem.* 266:20803–20809.

West, J. W., D. E. Patton, T. Scheuer, Y. Wang, A. L. Goldin, and W. A. Catterall. 1992. A cluster of hydrophobic amino acid residues required for fast Na(+)-channel inactivation. *Proc. Natl. Acad. Sci. U.S.A.* 89: 10910–10914.

Yeh, J. Z., and T. Narahashi. 1977. Kinetic analysis of pancuronium interaction with sodium channels in squid axon membranes. *J. Gen. Physiol.* 69:293–323.